Preprints of the 19th World Congress
The International Federation of Automatic Control
Cape Town, South Africa. August 24-29, 2014

A Hierarchical Control Scheme for Smooth Transitions between Level Ground and Ramps with a Robotic Transtibial Prosthesis

Kebin Yuan, **Qining Wang**, **Jinying Zhu**, **Long Wang**

Intelligent Control Laboratory, College of Engineering, Peking University, Beijing 100871, China

Abstract: This paper presents a hierarchical control scheme for a robotic transtibial prosthesis to realize smooth locomotion transitions between level ground and ramps. The high level controller identifies current terrain with a fuzzy logic based method and decides the corresponding parameters for lower level controllers. The middle level controller detects different gait phases of one gait cycle on a specific terrain and decides which control method to be used for the current phase. Based on the identified terrain and gait phase, the low level controller performs damping control for controlled plantarflexion/dorsiflexion, and angle control for the swing phase. To evaluate the effectiveness of the proposed control scheme, we design and construct a robotic transtibial prosthesis prototype. Experimental results on normalized stance time, normalized peak ground reaction force, and center of pressure shift in anterior/posterior show improved gait symmetry and walking stability of an amputee subject on ramps with the proposed control scheme. A 17-s long trial that includes different terrains and terrain transitions indicates that the proposed scheme can realize smooth locomotion transitions between level ground and ramps.

1. INTRODUCTION

Current transtibial prostheses play an important role in below-knee amputees' locomotion. However, most commercial prostheses have two main limitations. The first limitation is that these prostheses are energetically passive and can not provide net positive work, which leads to the amputees' more metabolic energy consumption and asymmetrical gait patterns during level ground walking (Winter et al. (1988)). In addition, the prosthetic joint angles are fixed or can not be adjusted automatically. As a result, the amputees wearing these prostheses are unable to adapt to terrain variations and may suffer balance impairment or even falling when walk on ramps or stairs.

To deal with these limitations, a lot of efforts have been made during recent years. Different kinds of robotic or powered transtibial prostheses with adjustable joints and kinds of actuators have been developed, e.g. Sup et al. (2007); Hitt et al. (2007); Au et al. (2009); Zhu et al. (2013). Being able to provide net positive work and mimic behaviors of the sound limb, these new prostheses can improve the amputees' energy efficiency and make their gaits more natural during level ground walking. Besides level ground walking, researchers have extended the prosthesis research to other terrains. As for stair ambulation with powered prostheses, several studies have been published (Au et al. (2008); Hoover et al. (2013); Lawson et al. (2013)).

⋆ This work was supported by the National Natural Science Foundation of China (No. 61005082, 61020106005) and and the 2011 R&D Project of the Beijing Disabled Persons' Federation.
E-mail: Q. Wang (qiningwang@pku.edu.cn) and L. Wang (longwang@pku.edu.cn)

However, studies related to ramp ambulation with passive prostheses or robotic ones are both limited. Since the absence of the adjustable ankle joints, ramp ambulation with passive prostheses is difficult to realize and few investigations have been proposed (Vrieling et al. (2008)). As for ambulation with robotic prostheses, limited studies have been presented. For example, Fradet et al. (2010) evaluated the biomechanical effects of adaptation of the *Össur* Proprio-Foot on ramp ambulation in transtibial amputees. The prosthetic ankle was set to the neutral angle mode (to simulate passive prostheses) and the adapted mode, respectively. However, the adaption to ramps is realized by only adjusting the joint angle to a predefined position. In addition, Sup et al. (2009) developed a powered transfemoral prosthesis and proposed a control strategy for upslope walking. Experimental results indicate that the powered prosthesis with the upslope walking controller is able to reproduce kinematic characteristics of healthy upslope walking (Sup et al. (2011)). But the downslope walking as well as the transitions between level ground and ramps were not studied.

This paper presents a hierarchical control scheme for a robotic transtibial prosthesis to realize smooth locomotion transitions between level ground and ramps. Both terrain identification methods and control strategies for ramp ascent and ramp descent are presented. Experiments with a transtibial amputee showed that the proposed scheme enables the robotic prosthesis to mimic the behavior of the normal limb and brings about a more natural gait during locomotion on level ground and ramps.

The rest of this paper is organized as follows. Section 2 introduces the prosthesis prototype. Section 3 introduces the hierarchical control strategy. Experimental results are presented in Section 4. We conclude in Section 5.

2. PROSTHESIS PROTOTYPE

To investigate smooth transitions between level-ground walking and ramp ascending/descending, we designed and constructed a robotic transtibial prosthesis with an ankle joint, named PKU-RoboTPro, short for ROBOtic Transtibial PROsthesis, Peking University. The prototype is shown in Fig. 1(a) and the mechanical structure is shown in Fig. 1(b). The model of the ankle joint can be simplified as a three-bar mechanism which comprises bars a, b, and c, and hinges, A, B, and C. To visualize the model, a can be seen as the foot, b as the shank, and C as the ankle joint. c is a customized bar made up of a motor-driven ball screw transmission. Its length can be changed by the motor and the length change is transformed into the joint rotation by the three-bar mechanism. The DC motor is a $50W$ brushless DC motor from Maxon (EC 45 - 50W), equipped with a 5.8:1 reduction gearbox. The range of the ankle joint is from 25° in dorsiflexion to 25° in plantarflexion. The total weight of the prosthesis (excluding the Li rechargeable battery) is $1.3kg$. Note that for prosthesis design, we have to strike a balance between the power and weight. As for this light-weight prosthesis, the motor power is 50 W and the theoretical peak torque of the ankle is around 60 Nm. Though the ankle is not powerful enough for fast walking, it can provide net positive work during low-speed motions.

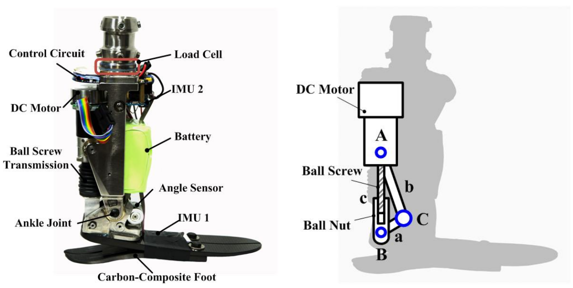

(a) (b)

Fig. 1. (a) The prototype of the proposed prosthesis (PKU-RoboTPro). (b) Ankle model, simplified as a three-bar mechanism.

Three kinds of sensors are installed on the prosthesis including the load cell, the angle sensor, and the inertial measurement unit (IMU), as shown in Fig. 1(a). The load cell (Interface LBS) has a measurement range of 0-250 lbf and is used to detect the interaction force between the residual limb of the amputee and the prosthesis. The absolute angle sensor (Angtron-RE-25) is used to measure the ankle angle with a 0-360 ° range and 12-bit resolution. Two IMUs are used to measure the inclination angle and other inertial information such as the acceleration and the rotation rates. One IMU is installed on the upper surface of the foot, and the other is installed on the shank of the prosthesis. Each IMU has an embedded tri-axis gyroscope and a tri-axis accelerometer. The gyroscope has a full-scale range of ± 2000 $°/s$ and a resolution of 0.06 $°/s$ while the accelerometer has a full-scale range of ± 16 g and a resolution of 0.5 mg.

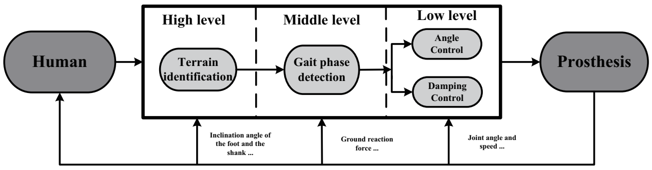

Fig. 2. The proposed hierarchical control scheme for the robotic prostheses.

3. HIERARCHICAL CONTROL SCHEME

To realize stable locomotion on ramps and smooth transition between level ground and ramps, a hierarchical control scheme is proposed, as shown in Fig. 2. The high level controller identifies the current terrain as well as terrain transitions and decides the corresponding parameters for the lower level controllers. The middle level and low level controller forms a finite-state controller (Yuan et al. (2010)). The middle level controller detects different gait phases of one gait cycle on a specific terrain and decides which control method to be used for the current phase. Based on the terrain and gait phase information, the low level controller then performs a specific control method.

3.1 High Level – Terrain Identification

Two features are selected to identify level ground (LG), ramp ascent (RA), and ramp descent(RD). One is the foot inclination angle at mid-stance, and the other is the maximal shank inclination angle during swing. These features are selected for two reasons. First, the features vary a lot between level ground and ramps, and can be easily used to distinguish these terrains. Second, the selected features are convenient to measure with just two IMUs and a force sensor.

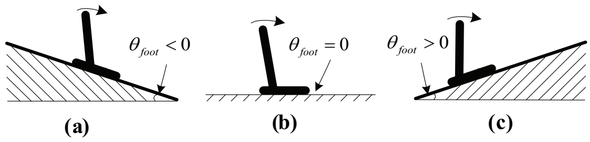

Fig. 3. Foot inclination angle at mid-stance.

Foot Inclination Angle at Mid-stance Foot inclination angle refers to the relative angle between the foot and the horizontal plane. This angle is defined to be zero when the foot is placed on the level ground, positive when foot rotates counterclockwise and negative when foot rotates clockwise. Mid-stance is defined as the moment $t_0 + 0.5T$, where t_0 refers to the start moment of the stance phase, and T refers to the period of last stance. At mid-stance, the foot is parallel to the terrain surface and the foot inclination angle (θ_{foot}) is equal to the terrain surface inclination angle. These angles of level ground and stairs are quite different from those of ramps, and can be used to distinguish different terrains, as shown in Fig. 3.

Maximal Shank Inclination Angle during Swing Shank inclination angle refers to the shank angle relative to the vertical plane. We define that the angle is zero when the shank is perpendicular to the horizontal ground, positive if the knee joint extends to the forward direction and negative if the knee joint flexes to the backward direction. The

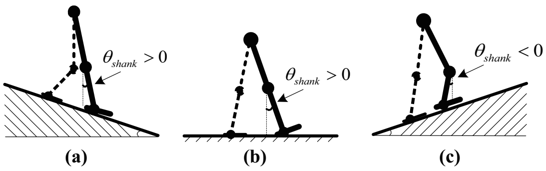

Fig. 4. Maximal shank inclination angle (θ_{shank}) during swing. θ_{shank} of ramp ascent is the minimum while that of the level ground is the maximum.

maximal shank inclination angle occurs at the moment close to the first foot strike and varies on different terrains, as shown in Fig. 4.

Based on the features, a fuzzy logic based identification method is used to identify different terrains. Detailed information can be found in our recent study (Yuan et al. (2013)).

3.2 Middle Level – Gait Phase Detection

The main subdivisions of one gait cycle are the stance phase when the foot is on the ground and the swing (SW) phase when the foot is off the ground. The stance phase of level ground walking can be further divided into three subphases: controlled plantar flexion (CP), controlled dorsiflexion (CD), and powered plantar flexion (PP) (Palmer. (2002)). Gait cycle of ramp ascent/descent can be divided in the same way (McIntosh. (2006)). In this paper, as the prosthesis is not powerful enough to provide sufficient net positive work, the PP phase is not detected. As a result, the stance phase consists of CP and CD only.

The gait phase is detected with the interaction force measured by the load cell and the ankle angle measured by the angle sensor. Stance phase is determined if the interaction force is continuously greater than a predefined threshold value for three sampling points. On the contrary, swing phase is determined if the interaction force is continuously less than the threshold value for three sampling points. During stance, CP is determined if the ankle angle decreases and CD is determined if the ankle angle increases.

The human ankle provides different functions during different phases of one gait cycle (Gates. (2004)). During CP and CD, the ankle absorbs the foot strike shock, stores the kinetic energy of human walking, and enables the body's center of gravity to move forward smoothly. During PP, the ankle provides net positive work to propel the body upward and forward. During SW, the ankle behaves as a position source to achieve foot clearance and reset the ankle to the equilibrium position. As is mentioned before, the motor of our prosthesis is not powerful enough to provide sufficient net positive work during PP, the proposed control strategy mainly concerns the ankle behavior during CP, CD, and SW phase.

Damping control For CP and CD phase, the ankle is usually modeled as a nonlinear spring with variable stiffness (Sinitski et al. (2011)). To mimic this function without spring, the prosthesis motor has to provided a resistive torque to prevent the ankle from plantar-flexing or dorsi-flexing too quickly, which is a waste of electric energy. To deal with this limitation, a damping control method is proposed based on the motor characteristics.

As is known to us, a motor can behave as a generator when the motor rotates, and the rotation will generate an induced voltage E_a,

$$E_a = C_e \phi n \tag{1}$$

where C_e refers to the electromotive constant, ϕ refers to the magnetic field intensity, and n refers to the motor speed.

If the motor terminals are shorted, the induced voltage will cause a current I_a, which can be estimated by

$$I_a = \frac{E_a}{R} \tag{2}$$

where R refers to the motor terminal resistance.

I_a will produce a braking torque τ_b that prevents the motor from rotating,

$$\tau_b = C_T \phi I_a = \frac{C_T C_E \phi^2}{R_a} n \tag{3}$$

where C_T refers to the motor torque constant.

From equation (3) we can see that the braking torque τ_b is proportional to the motor speed n. As the motor terminal resistance R_a is usually very low, the resulted braking torque τ_b will be very large once the motor rotates.

According to the rotation kinetics, the ankle motion during CP and CD phase could be described by

$$\tau_m - \tau_f - k\tau_b = I\ddot{\theta} \tag{4}$$

where τ_m refers to the rotation torque caused by the body mass, τ_f refers to the friction torque caused by the mechanical transmission, k refers to the proportional factor between the motor output torque and the resulted ankle joint torque, I refers to the rotational inertia of the shank, and θ refers to the ankle joint angle.

As the friction torque τ_f is much smaller than τ_m, τ_m will drive the ankle joint to rotate quickly without τ_b. If the motor terminals are shorted, the braking torque τ_b will be quite large once the joint rotates, and the resulted $\ddot{\theta}$ will decrease to a small value, so is the rotation angular rate $\dot{\theta}$. In this way, the prosthesis motor utilizes the human kinetic energy during walking to produce braking torque and does not consume any electric energy during stance.

If we switch on/off the motor terminal short with a pulse width modulation (PWM) signal, the braking torque during the switch-on period will be very large and the ankle joint can only rotate at a very low speed, while the braking torque during the switch-off period will be very small and the joint can rotate quickly. With an appropriate on/off frequency, the braking torque will be positively correlated with the duty cycle (D) of the PWM signal and the resulted equivalent braking torque (τ_{eb}) could be approximated as

$$\tau_{eb} = DK\dot{\theta} \tag{5}$$

where K is the proportional factor between the motor output torque and the resulted ankle joint torque.

The damping controller of the CP phase is designed to be:

$$D_1 = a_1(1 - 0.5(\tanh(s_1(\theta - \theta_{d1})) + 1)) \tag{6}$$

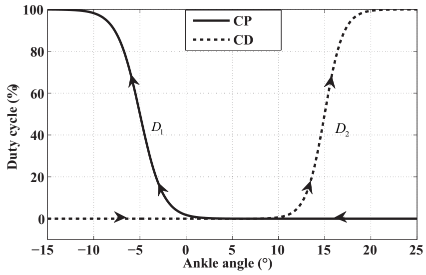

Fig. 5. Damping control function of CP and CD phase. $a_1 = a_2 = 100, s_1 = 0.4, s_2 = 0.5, \theta_{d1} = -5, \theta_{d2} = 15$.

where a_1 is the scale factor that constraints the maximal damping value, θ_{d1} is the threshold plantarflexion angle, θ is the current joint angle, s_1 is the sensitivity factor that decides the slope of the function and the resulted D_1 is the duty cycle of the PWM signal that controls the motor terminal short.

Similarly, the controller of the CD phase is designed as:

$$D_2 = 0.5a_2(\tanh(s_2(\theta - \theta_{d2})) + 1) \quad (7)$$

where θ_{d2} is the threshold dorsiflexion angle. The damping control functions are shown in Fig. 5.

3.3 Low Level – Damping/Angle Control

For the stance phase, θ_{d1} and θ_{d2} are set to be the maximal plantarflexion and maximal dorsiflexion angle, respectively. The dampings during early CP and CD phase are relatively small, which enable foot-flat and smooth progression of the body's center of gravity. As the joint angle approaches the maximal threshold angles, the damping will increase at a speed decided by s_1 and s_2, respectively.

Angle control For the swing phase, the ankle behaves as the position source and a Proportional-Derivative (PD) angle/position controller is designed to reset the ankle angle to the equilibrium position θ_{d0}.

Table 1. Control parameters

	Equilibrium $\theta_{d0}(degree)$	Plantarflexion θ_{d1} (degree)	Dorsiflexion θ_{d2} (degree)
Level ground	0	-5	12
Ramp descent	-3	-12	15
Ramp ascent	10	0	18

The structure of the low level controller is shown in Fig. 6 and control parameters of different terrains are shown in Table. 1. θ_{d1} and θ_{d2} set the ankle angle ranges during stance while θ_{d0} sets the equilibrium ankle angle during swing.

4. EXPERIMENTAL RESULTS

4.1 Subjects and Experiment Protocol

One transtibial amputee subject participated in the experiments to verify the effectiveness of the proposed control strategy. The amputee subject is 1.70m in height, 71 kg in weight and it has been eight years since the amputation. The subject has worn his current prosthesis (a 25-cm Otto Bock 1S90 foot) for three years and is experienced at prosthesis ambulation.

The experiments consisted of two sections. The first section was to test if the proposed control method could improve the amputee's gait symmetry and walking stability. In this section, the subject was firstly required to perform level ground walking, ramp descent, and ramp ascent with his passive prosthesis, respectively. Locomotion on each terrain was repeated for ten times. After that, the same locomotion was repeated with the robotic prosthesis for the same times. A force plate (footscan^{TM} 2D 2m plate, produced by RSscan International) was used to measure the ground reaction force (GRF) applied on the prosthetic foot as well as the intact foot. To testify the improvements of the proposed method, three indicators related to the walking stability - normalized stance time, normalized peak force, and center of pressure shift in anterior/posterior (Kendell et al. (2010)), was calculated based on the GRF measurements.

- *Normalized stance time.* Stance time refers to the period when the foot is on the ground and the stance time of both feet is expected to be equal. As the walking speeds of different trials vary, the stance time of both feet is normalized by the stance time of the intact foot of the same trial.
- *Normalized peak GRF.* Peak GRF refers to the maximal GRF during stance, and it is associated with the impact on the residual limb. Too large peak GRF may lead to unstable and asymmetric gaits. As the peak GRF varies with walking speeds and terrains, it is normalized by the average GRF value of the stance time.
- *Center of pressure (CoP) shift in anterior/posterior (AP).* During locomotion on different terrains, the human ankle rotates to enable the body's center of gravity to move smoothly from the posterior to the anterior, and the movement could be reflected by the GRF.

The second section was to test if the proposed control method could bring about smooth transition between level ground and ramps. The subject stood still at the beginning, and then performed level-ground walking, ramp descent, level-ground walking, standing, turning around, level-ground walking, ramp ascent, level-ground walking, and ended with standing again. The length of the ramp is $2.1m$ and the inclination angle is around $16.5°$. The interaction force, shank inclination angle, foot inclination angle, and ankle angle was recorded to testify the effectiveness of the proposed method. These locomotion information was sampled at 100 Hz, and the raw data was low-pass filtered by a three-order butterworth filter with a cut-off frequency of 5 Hz. During the experiment, the prosthesis was powered with a battery placed in a bag, and the sampled data was sent to the computer wirelessly by a transmitter, as shown in Fig. 7.

4.2 Results

The gait symmetry indicators calculated by the GRF measurements are shown in Fig. 8. As for the normalized stance time, the intact foot always has a greater value than the prosthetic one on different terrains. For LG,

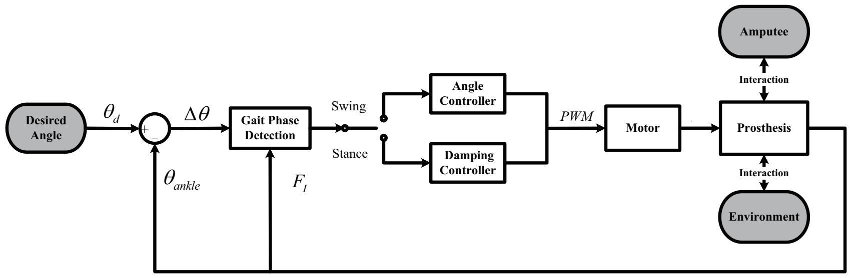

Fig. 6. The structure of the proposed low level controller.

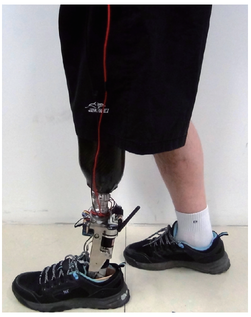

Fig. 7. The amputee subject with the proposed transtibial prosthesis.

there is no significant difference between the passive and the robotic prosthesis. For RD and RA, however, the robotic prosthesis brought about improvements of 13.0% and 13.7%, respectively. As for the normalized peak force, the robotic prosthesis reduced the peak values of both feet on all the three terrains, and the improvement of the intact foot during ramp descent was the largest. As for the CoP shift in AP direction, the shifts of both feet on LG were quite similar. But for RD and RA, the robotic prosthesis increased the CoP shifts significantly. These results show that the proposed control strategy for the robotic prosthesis could improve the amputee's walking stability as well as the gait symmetry.

Experimental results of the continuous locomotion transition between level ground and ramps are shown in Fig. 9. The subject stood still at the beginning. The first step was the level ground walking, which was identified at midstance when the foot inclination angle was around zero. As was controlled, the dorsiflexion angle of level ground was large while the plantarflexion angle was quite small. During the second step the terrain transited to ramp descent and the transition was detect at the end of the swing phase of the first step for the maximal shank inclination angle during swing is quite different from that of level ground walking. During ramp descent, the plantarflexion angle was increased to enable the foot-flat of the amputee. The controlled dorsiflexion angle should have increased too, but as the step length of the amputee was quite small, the resulted dorsiflexion angle was relatively small too. Transition to level ground was detect at the end of the third step and the controller preformed level ground walking for the fourth step again. After that, the subject stood still and then turned around. As the standing and turning around periods was not studied in this paper, they were depicted with dashed line in the figure. The fifth step started with level ground again, and transited to ramp ascent at the end of this step. During ramp ascent, the dorsiflexion angle of the ankle was quite large, which enables foot-flat and smooth locomotion of the body's center of gravity. After two steps of ramp ascent, the terrain transited to level ground again at the end of the seventh step. During the whole experiment period, the amputee did not experience balance impairment and he felt that it was more comfortable with the robotic prosthesis than the passive one to move between level ground and ramps.

As the prosthesis was unable to provide sufficient assistive torque during PP, the ankle angle is different from that of the able-bodied and that with a powered prosthesis (Sup et al. (2011)). But the extended angle motion range and damping control did improve the amputee's gait symmetry and walking stability compared with the passive prosthesis.

5. CONCLUSION

This paper proposed a hierarchical control scheme for a robotic transtibial prosthesis to realize smooth locomotion between level ground and ramps. Experimental results of a transtibial amputee subject showed improved walking stability and gait symmetry on ramps. A 17-s long trial that includes different terrains and terrain transitions is also presented to verify that the proposed control scheme can realize smooth locomotion between level ground and ramps. Future work includes the improvements of the proposed method to make the amputee's gait more symmetric, experiments with more amputees, and the application to more kinds of terrains.

REFERENCES

S. K. Au, M. Berniker, and H. Herr. Powered ankle-foot prosthesis to assist level-ground and stair-descent gaits. *Neural Networks*, (21):654-666, 2008.

S. K. Au, J. Weber, and H. Herr. Powered ankle-foot prosthesis improves walking metabolic economy. *IEEE Trans. Robotics*, 25(1):51-66, 2009.

L. Fradet, M. Alimusaj, F. Braatz, and S. I. Wolf. Biomechanical analysis of ramp ambulation of transtibial amputees with an adaptive ankle foot system. *Gait & Posture*, 32:191-198, 2010.

D. H. Gates. Characterizing ankle function during stair ascent, descent, and level walking for ankle prosthesis and orthosis design. Masters thesis, Department of Biomedical Engineering, Boston University, Boston, 2004.

J. Hitt, T. Sugar, M. Holgate, R. Bellman, and K. Hollander. Robotic transtibial prosthesis with biomechanical energy regeneration. *Industrial Robot*, 36(5):441-447, 2009.

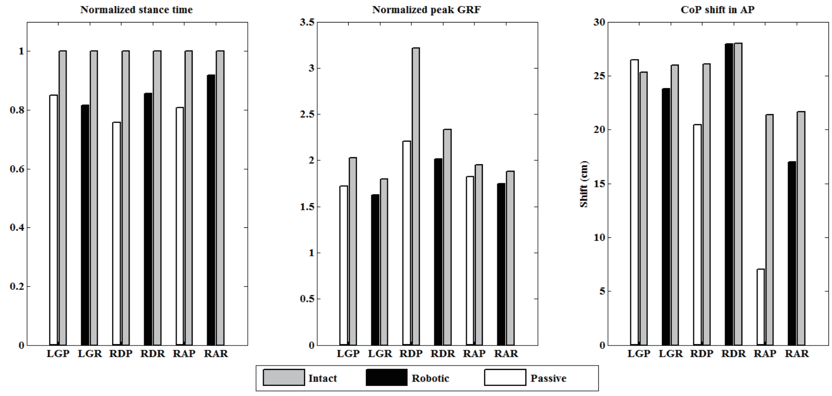

Fig. 8. Gait symmetry indicators with passive and robotic prostheses on different terrains. As for the label of x-axis, the letter LG, RD, and RA refers to level ground, ramp descent, and ramp ascent, respectively. The following letter P and R refers to passive and robotic, respectively. For example, "LGP" refers to level ground walking with the passive prosthesis while "LGR" refers to level ground walking with the robotic prosthesis.

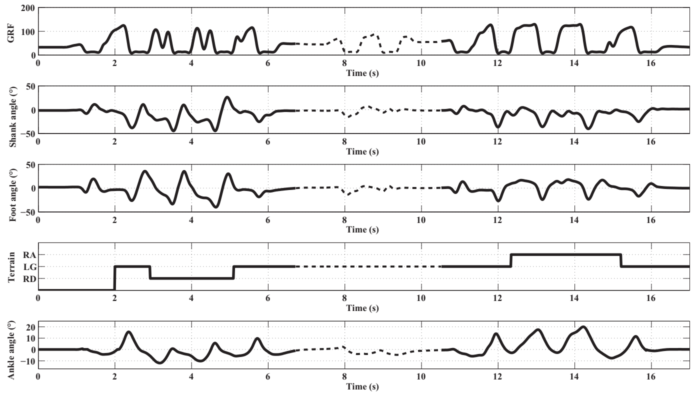

Fig. 9. Real-time continuous control strategy performance for 17-s long trial. The standing and turning around period was not included and was depicted with the dash line.

C. D. Hoover, G. D. Fulk, and K. B. Fite. Stair ascent with a powered transfemoral prosthesis under direct myoelectric control. *IEEE/ASME Trans. Mechatronics*, 18(3):1191-1200, 2013.

C. Kendell, E. D. Lemaire, N. L. Dudek, and J. Kofman. Indicators of dynamic stability in transtibial prosthesis users. *Gait & Posture*, 31:375-379, 2010.

B. E. Lawson, H. A. Varol, A. Huff, E. Erdemir, and M. Goldfarb. Control of stair ascent and descent with a powered transfemoral prosthesis. *IEEE Trans. Neural. Syst. Rehabil. Eng.*, 21(3):466-473, 2013.

A. S. McIntosh, K. T. Beatty, L. N. Dwan, and D. R. Vickers. Gait dynamics on an inclined walkway. *J. Biomech.*, 39:2491-2502, 2006.

M. Palmer. Sagittal plane characterization of normal human ankle function across a range of walking gait speeds. Master's thesis, Department of Mechanical Engineering, Massachusetts Institute of Technology, Boston, 2002.

E. H. Sinitski, A. H. Hansen, and J. M. Wilken. Biomechanics of the ankle-foot system during stair ambulation: Implications for design of advanced ankle-foot prostheses. *J. Biomech.*, 45:588-594, 2011.

F. Sup, A. Bohara, and M. Goldfarb. Design and control of a powered transfemoral prosthesis. *Int. J. Robot. Res.*, 27(2):263-273, 2008.

F. Sup, H. A. Varol, J. Mitchell, T. J. Withrow, and M. Goldfarb. Preliminary evaluations of a self-contained anthropomorphic transfemoral prosthesis. *IEEE/ASME Trans. Mechatronics*, 14(6):667-676, 2009.

F. Sup, H. A. Varol, and M. Goldfarb. Upslope walking with a powered knee and ankle prosthesis: initial results with an amputee subject. *IEEE Trans. Neural. Syst. Rehabil. Eng.*,, 19(1):71-78, 2011.

A. H. Vrieling, H. G. van Keeken, T. Schoppen, E. Otten, J. P. K. Halbertsma, A. L. Hof, and K. Postema. Uphill and downhill walking in unilateral lower limb amputees. *Gait & Posture*, 28(2):235-242, 2008.

D. A. Winter and S. E. Sienko. Biomechanics of below-knee amputee gait. *J. Biomech.*, 71(5):272-278, 1992.

K. Yuan, J. Zhu, Q. Wang, and L. Wang. Finite-state control of powered below-knee prosthesis with ankle and toe. *Proc. of the 18th IFAC World Congress*, pages 2865-2870, 2011.

K. Yuan, S. Sun, Z. Wang, Q. Wang and L. Wang. A fuzzy logic based terrain identification approach to prostheses control using multi-sensor fusion. *Proc. of the IEEE Int. Conf. Robotics and Automation*, pages 3361-3366, 2013.

J. Zhu, Q. Wang, and L. Wang. On the design of a powered transtibial prosthesis with stiffness adaptable ankle and toe joints. *IEEE Trans. Industrial Electronics*, 61(9):4797-4807, 2014.